

NASA Contractor Report 4319

First Evaluation of the Main
Parameters in the Dynamics
of the Small Expendable
Deployer System (SEDS)
for a Tethered Satellite

Luigi De Luca

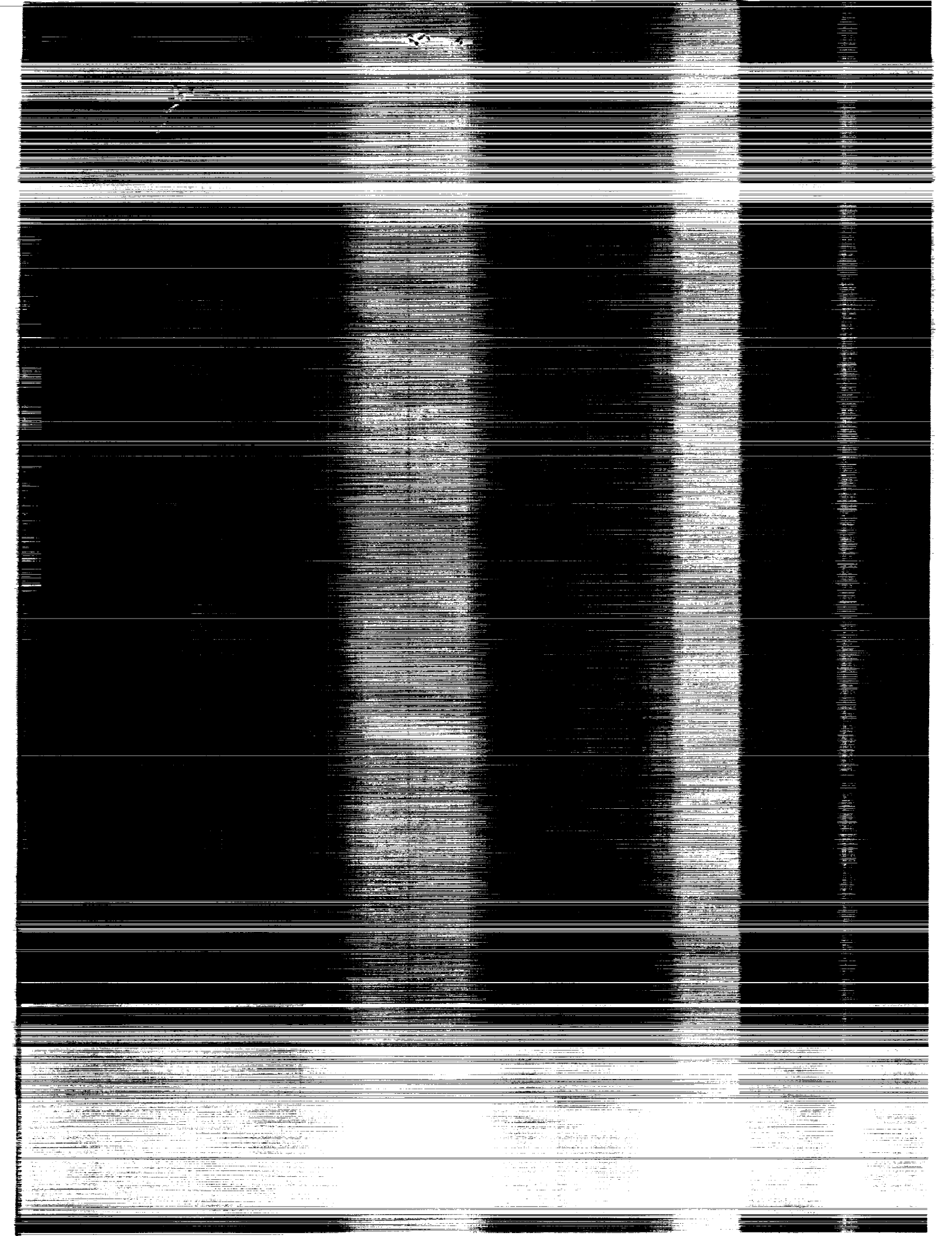
CONTRACT NAS1-18458
OCTOBER 1990

(NASA-CR-4319) FIRST EVALUATION OF THE MAIN
PARAMETERS IN THE DYNAMICS OF THE SMALL
EXPENDABLE DEPLOYER SYSTEM (SEDS) FOR A
TETHERED SATELLITE Contractor Report, 4 Aug.
- 2 Sep. 1988 (George Washington Univ.)

N91-10096

H1/15 Unclas
0310629





NASA Contractor Report 4319

First Evaluation of the Main
Parameters in the Dynamics
of the Small Expendable
Deployer System (SEDS)
for a Tethered Satellite

Luigi De Luca
The George Washington University
Joint Institute for Advancement of Flight Sciences
Hampton, Virginia

Prepared for
Langley Research Center
under Contract NAS1-18458

NASA

National Aeronautics and
Space Administration
Office of Management
Scientific and Technical
Information Division

1990



Abstract

The dynamics of the motion of the Small Expendable Deployer System (SEDS) is studied by using a simplified model in which no external forces (except the gravity gradient field) are applied on the tethered body and the tether is assumed massless. The dynamics of SEDS operation is modeled as a sequence of two phases: the deployment phase and the swing phase. For the first one the velocity dependent forces are found to force the tether forward from the local vertical. When the deployment ends, Coriolis effects vanish and the swing phase begins, which is characterized by a wide free libration. The time duration as well as velocity, acceleration and tension of the tethered body are estimated for both deployment and swing phases.

Nomenclature

a	transverse acceleration
Fr	Froude number, $V^2/3\Omega^2r^2$
g	gravity acceleration
L	total tether length
M	mass
r	distance from the orbital center
\dot{r}	radial velocity
\ddot{r}	radial acceleration
t	time
T	tension
V	velocity
θ	in-plane angle
$\dot{\theta}$	in-plane angular velocity
$\ddot{\theta}$	in-plane angular acceleration
ϕ	out-of-plane angle
$\dot{\phi}$	out-of-plane angular velocity
$\ddot{\phi}$	out-of-plane angular acceleration
τ	nondimensional time, $\tau = \frac{t\Omega}{2\pi}$
Ω	orbital angular velocity

Subscripts

d	deployment
m	maximum value
p	payload
r	radial
s	swing
ss	steady state
t	tether
o	initial value at deployment beginning
θ	in-plane
ϕ	out-of-plane

Introduction

This report describes the work done at NASA Langley Research Center during the period from August 4, 1988, to September 2, 1988, to model and study the dynamics associated with the use of tethered satellites deployed downward from a Space Transportation System (STS) or an ELV (Expendable Launch Vehicle) in order to obtain aerothermodynamic and atmospheric science data, as well as data about the dynamics of the tethered system itself.

The "Tethered Wind Tunnel" concept has been established and has been shown to be a valuable adjunct to other proposed flight programs to obtain aerothermodynamic and atmospheric data at altitudes between 50 and 150 km [1]. The second Tethered Satellite System (TSS-2) [2], the Shuttle Tethered Aerothermodynamic Research Facility (STARFAC) [3] and the Shuttle Continuous Open Wind Tunnel (SCOWT) [4], in particular, have the additional capability of obtaining steady-state data over the period of one or more orbits at a sustained altitude. However, both TSS/SCOWT and STARFAC are relatively large and sophisticated systems. In addition, the design of the satellite and of the deployer systems and the mission profiles are dictated by safety and operational constraints of STS, so that flight opportunities may be limited. This circumstance led to the definition of a simplified system consisting of a sacrificial satellite to be deployed as a secondary payload from an ELV (such as a Delta II), or as a primary payload on a smaller ELV. This simplified system is generally referred to as the Tethered Dynamics Explorer (TDE), or Tethered Atmospheric Probe (TAP) [5], a non-recoverable smaller satellite for obtaining data describing deployment dynamics, tether deployment rate and shape, tether tension, acceleration of the satellite, and other engineering and science data. These data might also be useful in defining the TSS-2 mission; however, the flight profiles will have little similarity to that of the TSS, hence, they will be applicable only in a generic sense.

This work, which was carried out in a cooperative NASA/ASI (Italian Space Agency) program about deployment and retrieval of tethered satellites, dealt with the study of the dynamics of the above described systems. It moved in two directions. On one hand, a detailed modeling, performed by using sophisticated general-purpose computer codes, has been approached. In particular, the use of the SKYHOOK program [6] has been studied. On the other hand, in order to define the order of magnitude of the main parameters affecting the dynamics of the DELTA II—Small Expendable Deployer System (SEDS) Flight Experiment [7], a simplified form of the motion equations has been derived and studied. Results and recommendations are presented.

In this report, part I describes the study performed using the SKYHOOK program; part II shows the derivation of the equations used to analyze the SEDS dynamics; and part III summarizes the results and includes recommendations.

Part I - Use of the SKYHOOK Computer Code

The study of the detailed dynamics of tethered systems dealt with a more in-depth knowledge of the SKYHOOK program [6], originally developed by the Smithsonian Astronomical Observatory, with the view of modifying codes to run on a 80386 class 20 MHz desktop computer. The SKYHOOK is a program of great generality which has the capability of analyzing a broad range of tether related scenarios. The STS and the satellite are represented by mass points, while the tether may be included in either mass or may be represented separately as a series of independently spaced mass points. Both thermal and elastic expansion of the tether, as well as solar and lunar perturbations, electrodynamic forces acting on the tether, and the effects of gravitational fields may be included. Moreover, atmospheric drag on the tether and the oblateness of the Earth may also be incorporated into the calculation. Analytical Mechanics Associates Inc. has modified the original version of SKYHOOK to include lower altitude calculations and a deployment routine specific to the STARFAC which more accurately deploys and retains the satellite at a target altitude for the required number of orbits.

The SKYHOOK mainly consists of the following routines:

- SKYHOOK - Main driver program which calls SKYIO to read data describing the run, and SKYIN2 which controls the integration of the equations of motion of the tether system.
- CONTRL - Computes the control-law tension on the wire segment being deployed. It is called by TENSION.
- DIFSUB - Integrates a set of N ordinary differential equation of first order, in our case the equation of motion plus temperature and charge equations. This routine, originally written by Gear, uses either an Adams-Moulton predictor—corrector method or a multistep method suitable for stiff systems. DIFSUB is called by SKYIN2.

- DIFFUN - Compute the right hand side of equations to be integrated. In particular, DIFFUN computes the sum of all forces acting on each segment of tether, the wire temperature (sub WIRTEMP) and the charge rate for electrodynamics (sub CHGRATE). DIFFUN is called by SKYIN2 and DIFSUB.
- DMPR - Points each data frame at requested frequency, specified by the variable DELT. It is called by SKYIN2.
- INITAL - Controls the computation of the initial conditions for a mass about to be deployed. It is called by SKYHOOK.
- INIT2 - Set up the initial state vector for a mass about to be deployed. INIT2 is called during the deployment phase by INITAL.
- MASSPTY - Read (and print) mass properties. It is called by SKYIO.
- READCS - Read (and print) the harmonic coefficients for the Earth gravity. READCS is called by SKYIO.
- SKYIN2 - This subroutine is the "true" SKYHOOK integrator. It controls the integration of the equations by calling DIFSUB, DIFFUN, DMPR. SKYIN2 contains two main loops. The inner loop performs the integration of the equations using time step H, the outer loop, ending every DELT time step, evaluates the different quantities to be printed and recomputes the nominal length of the wire segment just deployed according to the Hook law (sub NEWLO). SKYIN2 is called by SKYHOOK.
- SKYIO - Controls the reading of all input parameters at the beginning of the run. It is called by SKYHOOK.
- TENSION - Controls the computation of the tension on a section of the wire. If the tether is being deployed or retrieved, TENSION calls the proper control law tension for the segment being reeled out or pulled in, using CONTRL or RETRV, respectively. Tensions on the other sections are computed by using Hook law and damping with subroutine TETHER. TENSION is called by DIFFUN.

In order to better understand the overall operating conditions of the SKYHOOK program, and in particular to handle input, output and integrator modules, two runs have been carried out and the relative outputs studied. In the first run the downward deployment of a 20 km tether from an orbiter at 220 km of altitude has been simulated, using a 3-mass tether model. In the second run, a 4-mass tether model has been used to simulate the tether deployment from an orbiter at the same altitude of 220 km, down to 90 km. In both runs an equatorial orbit has been assumed.

Part II - Dynamics of Small Expendable Deployer System (SEDS)

The SEDS is based on two main concepts [8]: low tension deployment (which causes a large libration) and use of an expendable tether and satellite. In a typical SEDS operation, the payload is initially ejected from the STS by using a spring. Then the payload drifts away and pulls the tether out under very low tension. Actually, the system needs small tension adjustments to maintain the deployment schedule and a final braking phase reducing the deployment velocity at the end of the 20 km tether to prevent rebound of the end mass. At the end of the deployment phase a large in-plane (pitch) angle is obtained and, the effects related to the deployment rate vanish, a wide free libration ensues (swing phase). Finally, when the payload is about at a vertical position, the tether is cut and the payload is released. A detailed discussion about the main advantages related to the SEDS concept (low-tension deployment and expendable tether) is out of the aim of this report. It may be found in ref. [8]. In the following, in order to evaluate the order of magnitude of the main parameters characterizing the dynamics of SEDS deployment and swing phase, a rather simplified form of the equations of motion will be derived. It is believed that many of the most important aspects of the behavior of the SEDS dynamics can be predicted without resorting to complicated modeling and sophisticated computer codes.

II.1 - DEPLOYMENT PHASE

For this study, the following equations of motion [9] are derived:

$$\frac{\ddot{r}}{\Omega^2 r} = 3 \cos^2 \theta \cos^2 \phi + \left(1 + \frac{\dot{\theta}}{\Omega}\right)^2 \cos^2 \phi + \left(\frac{\dot{\phi}}{\Omega}\right)^2 - 1 \quad (1a)$$

$$\frac{\ddot{\theta}}{\Omega^2} = 2 \left(1 + \frac{\dot{\theta}}{\Omega}\right) \frac{\dot{\phi}}{\Omega} \operatorname{tg} \phi - \frac{3}{2} \sin 2\theta - 2 \frac{\dot{r}}{\Omega r} \left(1 + \frac{\dot{\theta}}{\Omega}\right) - \quad (1b)$$

$$\frac{\ddot{\phi}}{\Omega^2} = -\frac{\sin 2\phi}{2} \left[3 \cos^2 \theta + \left(1 + \frac{\dot{\theta}}{\Omega}\right)^2\right] + 2 \frac{\dot{r}}{\Omega r} \frac{\dot{\phi}}{\Omega} \quad (1c)$$

Figure 1 shows the rotating spherical coordinate system to which equations (1a-c) refer.

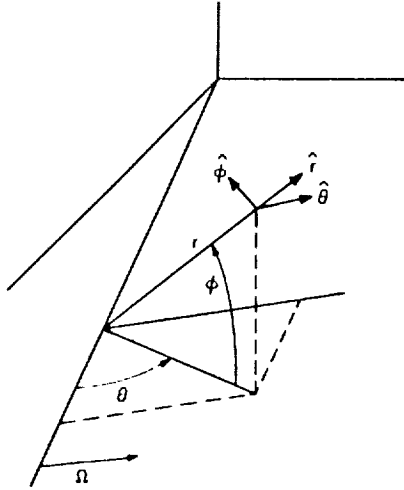


FIG. 1 Rotating Spherical Coordinate System [9]

where θ is the in-plane (pitch) angle, ϕ is the out-of-plane (roll) angle, and r is the distance from the orbital center. The orbital center O moves in a circular orbit at constant angular velocity Ω . No external forces are applied to the body. Equations (1) are valid for short tether lengths since they were derived by linearizing the gravity gradient force.

In order to obtain a simplified solution of system (1) during the deployment phase, the following assumptions are made. The validity of such assumptions (based on considerations drawn from ref. [10]) may be verified by an a-posteriori analysis. Then, if ϕ is small:

$$\sin \phi \simeq \phi$$

$$\cos \phi \simeq 1$$

$$\frac{\dot{\theta}}{\Omega} \ll 1 \quad \frac{\dot{\phi}}{\Omega} \ll 1$$

The system (1) becomes

$$\frac{\ddot{r}}{\Omega^2 r} = 3 \cos^2 \theta \quad (2a)$$

$$\frac{\ddot{\theta}}{\Omega^2} + 2\frac{\dot{r}}{\Omega r}\frac{\dot{\theta}}{\Omega} + \frac{3}{2} + \sin 2\theta = -2\frac{\dot{r}}{\Omega r} \quad (2b)$$

$$\frac{\ddot{\phi}}{\Omega^2} + 2\frac{\dot{r}}{\Omega r}\frac{\dot{\phi}}{\Omega} + (1 + 3\cos^2\theta)\phi = 0 \quad (2c)$$

During the deployment phase, in general, of course, θ is relatively large. However, when θ is small (initial instants of motion), eq. (2a) yields an exponential solution for r (i.e., $\frac{\dot{r}}{r} = \text{const}$) and eqs. (2b) and (2c) can be easily integrated. Moreover, in this case the solution of (2b) and (2c) is exponentially damped, and if such a damping is relatively fast as compared to the time required for the whole deployment, eq. (2b) can give a "good" prediction of the steady-state solution for the in plane angle θ . Then, eq. (2a) can be integrated again assuming $\theta = \text{const} = \theta_{ss}$. If θ is small we have:

$$\ddot{r} = 3\Omega^2 r \quad (3a)$$

$$\frac{\ddot{\theta}}{\Omega^2} + 2\frac{\dot{r}}{\Omega r}\frac{\dot{\theta}}{\Omega} + 3\theta = -2\frac{\dot{r}}{\Omega r} \quad (3b)$$

$$\frac{\ddot{\phi}}{\Omega^2} + 2\frac{\dot{r}}{\Omega r}\frac{\dot{\phi}}{\Omega} + 4\phi = 0 \quad (3c)$$

These equations are basically analogous to those obtained in refs. [10,11].

If $r(0) = r_o$ then eq. (3a) yields

$$r = r_o e^{\sqrt{3}\Omega t} \quad (4)$$

Note that $\dot{r}_o = \sqrt{3}\Omega r_o$. Another solution may be

$$\dot{r}_o = 0 \quad (5)$$

$$r = r_o \cos h(\sqrt{3}\Omega t) \quad (6)$$

$$\frac{\dot{r}}{r} = \sqrt{3}\Omega \operatorname{tgh}(\sqrt{3}\Omega t) \quad (7)$$

Assuming $\frac{\dot{r}}{r} = \sqrt{3}$, eq. (3b) becomes

$$\frac{\ddot{\theta}}{\Omega^2} + 2\sqrt{3}\frac{\dot{\theta}}{\Omega} + 3\theta = -2\sqrt{3} \quad (8)$$

For $\theta(0) = \theta_o = 0$, and $\dot{\theta}(0) = \dot{\theta}_o = 0$, eq. (8) yields

$$\frac{\theta - \theta_{ss}}{\theta_{ss}} = -(1 + \sqrt{3}\Omega t)e^{-\sqrt{3}\Omega t} \quad (9)$$

where $\theta_{ss} = -\frac{2\sqrt{3}}{3} = -1.15 \text{ rad} \simeq -66^\circ$.

In conclusion, during the deployment pitch, oscillations damp around the steady-state value of -66° . This means that the tether drifts forward with respect to the orbiter motion direction.

Assuming that the tether reaches the steady-state pitch angle very quickly, the deployment time t_d can be evaluated by integrating the equation

$$\frac{\ddot{r}}{\Omega^2 r} = 3\cos^2\theta_{ss} \quad (10)$$

Then we obtain

$$\tau_d = \frac{t_d \Omega}{2\pi} = \frac{1}{2\sqrt{3}\pi \cos 66^\circ} \ln \frac{L}{r_o} \quad (11)$$

where τ_d is the nondimensional deployment time and L is total length of the deployed tether. Assuming $L = 20$ km, $r_o = 200$ m [8], eq. (11) yields

$$\tau_d = 1.04 \quad (12)$$

If $\Omega = 1.156 \times 10^{-3}$ rad/s [12], we have

$$t_d \simeq 5655\text{s} \quad (13)$$

The deployment is accomplished in about 1 orbit. Of course this is not a detailed evaluation of the deployment time because, besides the assumptions made in deriving the basic equations, the “drift” phase only has been modeled, not including the “straighten” and the “braking” phases in which the tether tension (neglected in the previous analysis) is gradually raised. Since 10 minutes after the ejection the end mass should be over 200 m away from the orbiter [8], the total deployment time is estimated to be approximately 6200 s (r from 0 to 20 km). In ref. [8] the duration of the deployment, computed by the BEADSIM program (including straighten and braking effects) is 8100 s. For more consideration, see Part III: Conclusions and Recommendations.

As far as the evaluation of the acceleration is concerned, it has to be remembered that in our model the deployment trajectory is practically a straight line inclined 66° forward from the local vertical (see also [13]). The only component of the acceleration is then the radial one,

$$a_r = \ddot{r} = \frac{1}{2} \Omega^2 r_o e^{\sqrt{3}\Omega r} \quad (14)$$

Its maximum value for $t = t_d$ is

$$\ddot{r}_m = \frac{1}{2} \Omega^2 L = 1.34 \times 10^{-2} \text{ m/s}^2 \quad (15)$$

From results given by ref. [8], in the straighten part of deployment the maximum value of acceleration may be estimated to be one order of magnitude less than the value predicted by eq. (15). In conclusion, the (radial) acceleration in the deployment phase (at maximum) is estimated to be of the order of $10^{-3}g$ ($g = 9.81 \text{ m/s}^2$). It has to be noticed that the equation for the out-of-plane angle is of the same kind as that for the in-plane angle, however the forcing term is not present; accordingly during the deployment phase possible out-of-plane displacements are damped around zero angle. Then, in the present model the deployment trajectory may be considered totally contained in the orbital plane.

II.2 - SWING PHASE

The swing phase may be basically studied by using the equations of system (1a-c). It may be assumed that swing phase begins when the deployment is completed. In effect, during the deployment phase the velocity dependent forces due to the motion relative to the rotating orbital system (Coriolis forces) force the tether forward from the local vertical. When the deployment ends Coriolis effects vanish and the tether experiences a wide free libration (swing phase).

Under the same assumptions made to study the deployment phase, and putting $\dot{r} = 0$, eqs. (2b) and (2c) yield

$$\frac{\ddot{\theta}}{\Omega^2} = -3 \sin \theta \cos \theta \quad (16a)$$

$$\frac{\ddot{\phi}}{\Omega^2} = -4 \sin \phi \cos \phi \quad (16b)$$

Note that in the aim of decoupling the equations in the second equation, $\cos\theta \simeq 1$. Equations (16a-b) can also be derived by writing the equilibrium of the pendulum subjected to the gravity gradient field. For initial conditions

$$\theta = \theta_m \quad \dot{\theta} = 0$$

$$\phi = \phi_m \quad \dot{\phi} = 0$$

the solutions of eqs. (16a) and (16b) are

$$\frac{\dot{\theta}}{\Omega} = \pm\sqrt{3}\sqrt{\sin^2\theta_m - \sin^2\theta} \quad (17a)$$

$$\frac{\dot{\phi}}{\Omega} = \pm 2\sqrt{\sin^2\phi_m - \sin^2\phi} \quad (17b)$$

The oscillation period t_θ may be computed as

$$t_\theta = 4 \int_0^\theta m \frac{d\theta}{\dot{\theta}}$$

After resolving the integral, we have

$$\frac{t_\theta\Omega}{2\pi} = \frac{1}{\sqrt{3}} \left[1 + \left(\frac{1}{2}\right)^2 \sin^2\theta_m + \left(\frac{13}{24}\right)^2 \sin^4\theta_m + \left(\frac{135}{246}\right)^2 \sin^6\theta_m + \dots \right]$$

or

$$\frac{t_\theta\Omega}{2\pi} \simeq \frac{1}{\sqrt{3} \cos\theta_m}$$

The duration t_s of the swing phase is then $t_s = \frac{t_\theta}{4}$. In nondimensional form

$$\tau_s = \frac{t_s\Omega}{2\pi} = \frac{1}{4} \frac{1}{\sqrt{3} \cos\theta_m} \quad (18)$$

If $\theta_m = 66^\circ$

$$\tau_s = 0.23 \quad (19)$$

Equation (19) means that the swing phase is accomplished in about 1/4 of orbit. In other words

$$t_s \simeq 1250s \quad (20)$$

As far as the order of magnitude is concerned, results (19) or (20) are in agreement with those of refs. [8,12]. Once $\frac{\dot{\theta}}{\Omega}$ and $\frac{\dot{\phi}}{\Omega}$ have been calculated, they may be substituted into complete eqs. (1a-c) in order to evaluate tension T and accelerations. In the swing phase we have

$$T = 3M\Omega^2 L \left[\cos^2\theta \cos^2\phi - \frac{1}{3} + \frac{\cos^2\phi}{3} \left(1 + \frac{\dot{\theta}}{\Omega} \right)^2 + \frac{1}{3} \left(\frac{\dot{\phi}}{\Omega} \right)^2 \right]$$

and then

$$T = 3M\Omega^2 L \left\{ \cos^2\phi \left[\cos^2\theta + (\sin^2\theta_m - \sin^2\theta) \pm \sqrt{\frac{4}{3}(\sin^2\theta_m - \sin^2\theta)} \right] - \frac{1}{3} \sin^2\phi + \frac{4}{3} (\sin^2\phi_m - \sin^2\phi) \right\} \quad (21)$$

From eq. (21) it is possible to evaluate the tension T as a function of θ_m , ϕ_m and current θ and ϕ angles.

The most difficult situation occurs when $\phi = 0$. In this case:

$$T = 3M\Omega^2 L \left[\cos^2 \theta + (\sin^2 \theta_m - \sin^2 \theta) \pm \sqrt{\frac{4}{3} (\sin^2 \theta_m - \sin^2 \theta) + \frac{4}{3} \sin^2 \phi_m} \right]$$

If $\theta = 0$ (end of swing phase), $\theta_m = 66^\circ$ and $\phi_m = 30^\circ$, we have

$$T = 9.66M\Omega^2 L \quad (22)$$

Assuming $\Omega = 1.156 \times 10^{-3}$ rad/s, $M = 50$ kg, $L = 20$ km, (22) yields

$$T = 12.9N.$$

Note that [see eq. (21)] for high values of θ_m , and θ near in magnitude to θ_m , in the retrograde phase of a period the tether could become slack. This should not be the case in SEDS.

The results obtained for angular velocities, swing phase timing, and tension agree well with similar results of ref. [14]. Transverse acceleration components may be calculated from angular accelerations. In spherical coordinates it results [15]:

$$a_\theta = L\ddot{\theta} \cos \phi + 2L\dot{\theta}\dot{\phi} \sin \phi \quad (23a)$$

$$a_\phi = L\ddot{\phi} - \frac{L\dot{\theta}^2}{2} \sin 2\phi \quad (23b)$$

Of course, in the swing phase, $\dot{r} = 0$ and $r = L$. Then $\ddot{\theta}$ and $\ddot{\phi}$ are respectively

$$\ddot{\theta} = \Omega^2 \left[2 \left(1 + \frac{\dot{\phi}}{\Omega} \right) \frac{\dot{\phi}}{\Omega} \operatorname{tg} \phi - \frac{3}{2} \sin 2\theta \right] \quad (24a)$$

$$\ddot{\phi} = -\frac{\Omega^2}{2} \sin 2\phi \left[3 \cos^2 \theta + \left(1 + \frac{\dot{\theta}}{\Omega} \right)^2 \right] \quad (24b)$$

Putting (24a) into (23a) yields

$$a_\theta = \Omega^2 L \cos \phi \left[2 \frac{\dot{\phi}}{\Omega} \left(1 + 2 \frac{\dot{\theta}}{\Omega} \right) \operatorname{tg} \phi - \frac{3}{2} \sin 2\theta \right]$$

and, taking into account (17a) and (17b):

$$a_\theta = \Omega^2 L \cos \phi \left[\pm 4 \sqrt{\sin^2 \phi_m - \sin^2 \phi} \left(1 \pm 2\sqrt{3} \sqrt{\sin^2 \theta_m - \sin^2 \theta} \right) \operatorname{tg} \phi - \frac{3}{2} \sin 2\theta \right] \quad (25a)$$

In an analogous way it results

$$a_\phi = -\frac{\Omega^2 L}{2} \sin 2\phi \left[1 + 3 \cos^2 \theta \pm 2\sqrt{3} \sqrt{\sin^2 \theta_m - \sin^2 \theta} + 6 (\sin^2 \theta_m - \sin^2 \theta) \right] \quad (25b)$$

Let us examine (25a). Suppose ϕ_m is small, thus eq. (25a) becomes

$$a_\theta = \Omega^2 L \left[\pm 4 \sqrt{\phi_m^2 - \phi^2} \left(1 \pm 2\sqrt{3} \sqrt{\sin^2 \theta_m - \sin^2 \theta} \right) \phi - \frac{3}{2} \sin 2\theta \right]$$

The factor $\phi \sqrt{\phi_m^2 - \phi^2}$ is of order of ϕ^2 ; then the relation may be simplified as

$$a_\theta = -\frac{3}{2} \Omega^2 L \sin 2\theta \quad (26)$$

a_θ reaches its maximum value at $\theta = -\frac{\pi}{4}$: $a_{\theta \max} = \frac{3}{2} \Omega^2 L$. For $\Omega = 1.156 \times 10^{-3}$ rad/s and $L = 20$ km, $a_\theta \simeq 4.0 \times 10^{-2}$ m/s². For $\theta = 0$, $a_\theta = 0$. As far as the expression of a_ϕ is concerned, note that if $\phi = 0$, $a_\phi = 0$. If $\phi \neq 0$, assuming the plus sign in eq. (25b) during swing phase, the maximum value of a_ϕ is obtained when $\theta = 0$. (The tether is vertical, before cutting.) The absolute value is

$$a_\phi = \Omega^2 L \sin 2\phi (2 + \sqrt{3} \sin \theta_m + 3 \sin^2 \theta_m) \quad (27)$$

If $\theta_m = 66^\circ$, $a_\phi \simeq 6\Omega^2 L \sin 2\phi$. If $\phi = 15^\circ$, $a_\phi \simeq 8.0 \times 10^{-2}$ m/s². From these results it is evident that maximum transverse out-of-plane acceleration can be about 2 times the maximum value reached at $\theta = -\frac{\pi}{4}$ by the transverse in-plane acceleration.

However it is interesting to observe that for $\phi = 1^\circ$, $a_\phi = 5.6 \times 10^{-3}$ m/s², that is to say, that even in the presence of very small out-of-plane oscillations, the out-of-plane transverse acceleration is "only" one order of magnitude less than the maximum in-plane acceleration.

Part III - Conclusions and Recommendations

The dynamics of motion of an SEDS has been studied by using a simplified model in which no external forces (except the gravity gradient field) are applied on the tethered body and the tether is massless. Furthermore, due to the short tether length which is typical of SEDS, equations have been derived by linearizing the gravity gradient force. The dynamics of SEDS operation has been modeled as a sequence of two phases: the deployment phase and the swing phase. In the first one the velocity dependent forces due to tethered end mass motion relative to the rotating orbital system (Coriolis forces) force the tether itself forward from the local vertical. A wide in-plane angle is quickly reached practically at the beginning of the deployment. When the deployment ends, Coriolis effects vanish ($\dot{r} = 0$) and the swing phase begins, which is characterized by a wide free libration. The deployment phase has been studied assuming that the oscillations of the in-plane (pitch) angle quickly damp and a wide steady-state in-plane angle is attained practically instantaneously. Nevertheless, in order to evaluate such a steady-state angle, the linearized form of the in-plane motion equation has been solved (this equation generally is typical of a nonlinear oscillator with damping and driving terms proportional to \dot{r}/r). (This allowed us to evaluate the constant deployment angle to be about 66° from the vertical, forward with respect to the orbiter motion.) Accordingly, the deployment occurs at this constant in-plane angle for its whole duration.

Note that usually the payload is ejected with an initial velocity from the orbiter by means of a spring. Due to the particular environmental conditions experienced by the tethered mass, this mass does not "feel" instantaneously the gravity gradient field (allowing the tether to be deployed in a free-nul (or low) tension motion), but a certain delay occurs. To evaluate this delay we may use a modified form of Froude number

$$Fr = V^2 / g' L \quad (28)$$

where V and L are reference velocity and length and g' is the gravity gradient field acceleration:

$$g' = 3\Omega^2 r \quad (29)$$

Then

$$Fr = V^2/3\Omega^2r^2 \quad (30)$$

When the payload is ejected from the orbiter at velocity V , it feels the orbital dynamic effects if $F = 0$ [1]. Since $r = Vt$, eq. (30) gives

$$t = \frac{1}{\sqrt{3}\Omega} \quad (31)$$

If $\Omega = 1.156 \times 10^{-3}$ rad/s, $t = 500$ s. In conclusion, on timescales longer than about 10 minutes, orbital dynamic effects become significant. This result agrees with considerations made in ref. [8]. This means that, after payload ejection, in the first 500 s the deployment rate may be assumed constant, $\dot{r} = 0.4$ m/s (ref. [8]), and a distance $r = (0.4 \text{ m/s}) \times 500 \text{ s} = 200$ m is initially attained. From this instant eq. (10) applies. The deployed length, deployment rate, and acceleration are found to be respectively

$$r = r_o e^{\sqrt{3}\Omega(\cos 66^\circ)(t-t_o)} \quad (32)$$

$$\dot{r} = \sqrt{3}\Omega(\cos 66^\circ)r \quad (33)$$

$$\ddot{r} = 3\Omega^2(\cos 66^\circ)^2r \quad (34)$$

Note that eqs. (32), (33), and (34) overestimate r , \dot{r} , and \ddot{r} with respect to results given by ref. [8]. This is probably due to the fact that, in the presence of control tension and if the elasticity of tether material is included into the model, the time constant in eq. (32) is less than $\sqrt{3}$.

Maximum estimated acceleration is of order of 10^{-2} m/s² (or 10^{-3} g). At the end of the "straighten" phase ref. [8] estimates $\ddot{r} = 0(10^{-3} \text{ m/s}^2)$.

Deployment time (from $r = r_o$) is

$$\tau_d = \frac{t_d\Omega}{2\pi} = \frac{1}{2\pi\sqrt{3}\cos 66^\circ} \ln \frac{L}{r_o} \quad (35)$$

For $\Omega = 1.156$ rad/s the deployment is accomplished in about 1 orbit.

Note that the steady-state angle in ref. [8] is estimated to vary about from 65° to 72° at the end of the straighten phase. Steady-state value is reached in about (500 + 1000)s.

The swing phase has been assumed to start from $\theta = -66^\circ$. In order to study this phase the same model of deployment phase was used in which, of course, $\dot{r} = 0$.

Relationships for angular velocity and angular acceleration in in-plane and (if possible) out-of-plane motions have been derived. See eqs. (17a-b) and (24a-b). The swing duration is

$$\tau_s = \frac{t_s\Omega}{2\pi} = \frac{1}{4} \frac{1}{\sqrt{3}\cos \theta_m} \simeq 0.23 \text{ orbits, or } t_s = 1200 \text{ s} \quad (36)$$

A complete equation to evaluate the tension as a function of in-plane and out-plane angles is given by (21). When $\theta = 0^\circ$ (end of swing phase) it results

$$\text{If } \phi_m = \phi = 0^\circ \quad T \simeq 11.6 \text{ N} \quad (37)$$

$$\text{If } \phi_m = 30^\circ \text{ and } \phi = 0^\circ \quad T \simeq 12.9 \text{ N}$$

The result of eq. (37) is in excellent agreement with ref. [8]. From an analysis of eq. (21) it arises that for high values of θ_m , and θ near to θ_m in magnitude, in the retrograde phase of a period of oscillation, the tether could become slack. This should not be the case in SEDS.

Transverse in-plane and out-of-plane accelerations are given by eqs. (25a-b); a_θ is practically independent of out-of-plane motion and reaches its maximum value at $\theta = -\frac{\pi}{4}$: $a_\theta \text{ max} = \frac{3}{2}\Omega^2 L \simeq 4 \times 10^{-2} \text{ m/s}^2$; a_ϕ attains its maximum value when $\theta = 0^\circ$. This maximum value, for $\theta_m = -66^\circ$ and $\phi = 15^\circ$ is $a_\phi \text{ max} = 3\Omega^2 L$. Then, the maximum out-of-plane transverse acceleration could be about 2 times greater than the maximum value of in-plane transverse acceleration.

Note that most of the data from ref. [8] are taken from table 8.2.3.2, page 158, and are shown in Table 1.

TABLE 1. BEADSIM Summary Output File for First SEDS Experiment [8]

Time	NomLng	ActLng	TotRng	XRange	YRange	ActdL	RngRate	Tension
0	1	1	1	0	-1	0.40	0.40	0.011
300	115	115	115	-38	-109	0.37	0.38	0.011
600	231	231	231	-134	-189	0.40	0.40	0.011
900	355	355	355	-262	-239	0.42	0.42	0.011
1200	483	483	483	-402	-268	0.43	0.43	0.011
1500	610	610	610	-539	-284	0.42	0.42	0.011
1800	733	733	733	-669	-301	0.41	0.41	0.011
2100	861	861	861	-794	-331	0.44	0.44	0.011
2400	1005	1005	1005	-929	-384	0.53	0.53	0.012
2700	1185	1185	1185	-1090	-467	0.68	0.69	0.012
3000	1425	1425	1425	-1300	-583	0.92	0.92	0.013
3300	1743	1743	1743	-1581	-733	1.21	1.21	0.014
3600	2157	2157	2156	-1954	-912	1.54	1.55	0.015
3900	2677	2677	2676	-2434	-1113	1.91	1.92	0.018
4200	3312	3312	3310	-3030	-1330	2.30	2.30	0.021
4500	4060	4060	4057	-3746	-1557	2.68	2.68	0.025
4800	4922	4922	4918	-4580	-1790	3.05	3.05	0.030
5100	5896	5896	5888	-5527	-2028	3.43	3.41	0.037
5400	6979	6979	6966	-6583	-2279	3.78	3.78	0.045
5700	8172	8172	8155	-7745	-2554	4.17	4.15	0.056
6000	9483	9483	9462	-9016	-2870	4.58	4.57	0.071
6300	10930	10930	10905	-10409	-3253	5.07	5.06	0.096
6600	12533	12533	12509	-11937	-3739	5.63	5.65	0.136
6900	14322	14322	14304	-13618	-4375	6.29	6.33	0.212
7200	16320	16320	16310	-15446	-5238	7.00	7.03	0.375
7500	18482	18484	18481	-17318	-6451	7.12	7.13	1.104
7800	19770	19774	19774	-18032	-8116	1.60	1.59	1.940
8047	20000	20007	20007	-16993	-10560	0.57	0.58	4.002
8100	20000	20005	20005	-16538	-11256	0.23	0.24	2.873
8400	20000	20016	20015	-11899	-16094	0.02	0.01	7.812
8700	20000	20023	20023	-2769	-19831	0.01	0.01	11.614

EndSec ApsisAlt PeakTension @ sec BrakeWork Exposure Risk:3d>D
8700 35.63 km 11.620 new 8699 5788 j 16.57 KmHr 0.182%

Concluding Remarks

A first step to enhance the results obtained analytically is to integrate the same model [eqs. (1)] numerically. Then mass of tether, elasticity, and tension control law could be included (together with aerodynamic effects). To be investigated:

- 1) influence of T/M_p (T = tension, M_p = payload mass) on libration angle and range rate.
- 2) influence of M_t/M_p (M_t = tether mass) on tether curvature.
- 3) possible vibrational modes

Acknowledgments

The author wishes to acknowledge Dr. G. M. Wood of NASA LaRC whose support (human and material) was instrumental in performing the work reported herein.

References

1. Workshop Proceedings: Applications of Tethers in Space, NASA CP-2366, (1985).
2. Workshop Proceedings: Applications of Tethers in Space, NASA CP-2422, (1986).
3. Siemers, P. M., Wood, G. M., Wolf, H., Flanagan, P. F., and Henry, M. W.; "The Definition of the Shuttle Tethered Aerothermodynamics Research Facility," AIAA-85-1794 (1985).
4. Carlomagno, G. M., de Luca, L., Siemers, P. M., and Wood, G. M.; "Low Density Aerothermodynamic Studies Performed by Means of the Tethered Satellite System," Proc. 15th Int. Symp. Rarefied Gas Dynamics, 574, Grado, Italy (1986).
5. Wood, G. M. and Siemers, P. M., Squires, R. K. and Wolf, H., Carlomagno, G. M. and de Luca, L.; "Downward-Deployed Tethered Platforms for High Enthalpy Aerothermodynamic Research," AIAA-88-0688 (1988).
6. Kirschner, L. R.; "The SKYHOOK Program: a Software Program for a Tethered Satellite System," Contract NAS8-33691 (1980). (Available from Marshall Space Flight Center.)
7. Lemke, L. G., Rupp, C. C., Webster, W. J., and Wood, G. M.; "Early Tether Dynamics Flight Experiment," Proc. Second International Conference on Tethers in Space, NASA/PSN, Venice (Italy) (1987).
8. Carroll, J. A., and Alexander, C. M.; "SEDS. The Small Expendable Tether Deployment System," Final Report Phase II, Contract NAS8-35256 (1987). (Available from Marshall Space Flight Center.)
9. Arnold, D. A.; "The Behavior of Long Tethers in Space," J. Astron. Sc., Vol. 35, N. 1, (1987) pp. 3-18.
10. Misra, A. K. and Modi, V. J.; "A Survey on the Dynamics and Control of Tethered Satellite Systems," NASA/AIAA/PSN International Conference on Tethers in Space, Arlington (VA) (1986).
11. Rupp, C. C.; "A Tether Tension Control Law for Tethered Subsatellites Deployed Along Local Vertical," NASA TMX-66963, Marshall SFC (1975).

12. Rupp, C. C.; "Early Tether Dynamics Flight Experiments," in Space Tethers for Science in the Space Station Era, Conf. Proc. Vol. 14, Societa Italiana di Fisica, Bologna (Italy) (1987).
13. Von Flotow, A. H., and Williamson, P. R.; "Fast (3/4 Orbit) Deployment of a Tethered Satellite Pair to the Local Vertical," NASA/AIAA/PSN International Conference on Tethers in Space, Arlington (VA) (1986).
14. Carroll, J. A.; "Tether Fundamentals Presentation," Applications of Tethers in Space, NASA CP-2422, Vol. I, (1986) pp. 82-94.
15. Torby, B. J.; "Advanced Dynamics for Engineers," Holt, Rinehart and Winston (1984).



Report Documentation Page

1. Report No. NASA CR-4319		2. Government Accession No.		3. Recipient's Catalog No.	
4. Title and Subtitle First Evaluation of the Main Parameters in the Dynamics of the Small Expendable Deployer System (SEDS) for a Tethered Satellite			5. Report Date November 1990		
			6. Performing Organization Code		
7. Author(s) Luigi De Luca			8. Performing Organization Report No.		
			10. Work Unit No. 906-70-16-02		
9. Performing Organization Name and Address George Washington University Joint Institute for Advancement of Flight Sciences NASA Langley Research Center Hampton, VA 23665-5225			11. Contract or Grant No. NAS1-18458		
			13. Type of Report and Period Covered Contractor Report 8/4/88-9/2/88		
12. Sponsoring Agency Name and Address National Aeronautics and Space Administration Langley Research Center Hampton, VA 23665-5225			14. Sponsoring Agency Code		
			15. Supplementary Notes Langley Technical Monitor: George M. Wood Luigi De Luca: Now at Dipartimento di Energetica termofluidodinamica Università di Napoli		
16. Abstract The dynamics of the motion of the Small Expendable Deployer System (SEDS) is studied by using a simplified model in which no external forces (except the gravity gradient field) are applied on the tethered body and the tether is assumed massless. The dynamics of SEDS operation is modeled as a sequence of two phases: the deployment phase and the swing phase. For the first one the velocity dependent forces are found to force the tether forward from the local vertical. When the deployment ends, Coriolis effects vanish and the swing phase begins, which is characterized by a wide free libration. The time duration as well as velocity, acceleration and tension of the tethered body are estimated for both deployment and swing phases.					
17. Key Words (Suggested by Authors(s)) Tethered Satellite Dynamics			18. Distribution Statement Unclassified—Unlimited Subject Category 15		
19. Security Classif. (of this report) Unclassified		20. Security Classif. (of this page) Unclassified		21. No. of Pages 16	22. Price A03

